

## Effect of S segregation on the surface magnetism of Fe(100)

Giorgio Rossi

*Laboratorium für Festkörperphysik, Eidgenössische Technische Hochschule Zürich, CH-8093 Zürich, Switzerland*

Giancarlo Panaccione and Fausto Sirotti

*Laboratoire pour l'Utilisation du Rayonnement Electromagnetique, CNRS-CEA-MESR, F-91405 Orsay, France*

(Received 5 September 1995; revised manuscript received 18 December 1995)

Bulk impurities of the ferromagnetic transition metals segregate at the surface at moderate temperature and severely modify the surface magnetic properties. S segregation on Fe(100) produces a stable  $c(2 \times 2)$  reconstruction at 600 °C. We have measured the change of the magnetic properties of Fe(100) due to the formation of the  $c(2 \times 2)$ S surface by measuring the exchange coupling along a path perpendicular to the surface via the spin-wave stiffness and the relative change of the iron surface magnetic moment by photoemission magnetic dichroism experiments and spin-polarization measurements of the secondary yield. A stronger coupling between the  $c(2 \times 2)$ S surface and the bulk than for the clean Fe(100) free surface is found. Changes of the Fe 3*p* core hole magnetic splitting show that the surface magnetic moment of Fe is reduced by up to 20% upon S segregation with respect to the clean surface. Strong magnetic dichroism of the electron states just below the Fermi level indicates a filling of the surface minority spin band in the  $c(2 \times 2)$ S/Fe(100) surface relative to the clean Fe(100) surface. [S0163-1829(96)08229-X]

### INTRODUCTION

Surface magnetism differs from bulk magnetism due to the highly anisotropic environment of surface atoms which has important consequences on the electron states at the surface, and consequently on the exchange interaction. The magnetism of surfaces is characterized by different magnetic moments with respect to the bulk and by different exchange coupling to the other planes of the semi-infinite solid. Magnetism is most sensitive to surface contamination by chemisorbed atoms or atoms segregated from the bulk and one can speak of magnetic poisoning of a surface much in the same way as one does with respect to the hindering of the catalytic properties of transition-metal surfaces by impurities. The understanding of the surface magnetochemistry of iron is obviously important. Several experimental studies of the S adsorption or segregation on Fe(100) have been reported, based on low-energy electron diffraction (LEED),<sup>1</sup> work function measurements,<sup>2</sup> angular resolved photoemission (ARPES)<sup>3</sup> and on angle- and spin-resolved photoemission<sup>4,5</sup> spectroscopies of the extended electron states. In these papers the atomic order and the electron states of the  $c(2 \times 2)$ S/Fe(100) surface were measured and evidence was obtained of the presence of exchange splitting on S derived valence states, as well as of changes of the iron *d* bands with respect to the clean Fe(100) surface. First-principles band calculations for the  $c(2 \times 2)$ S/Fe(100) surface predicted a reduction of the surface magnetic moment of iron as a consequence of Fe 3*d*-S 3*p* band hybridization.<sup>6</sup>

In the present study we have measured the exchange coupling to the bulk for both the Fe(100) and  $c(2 \times 2)$ S/Fe(100) surfaces via the spin-wave stiffness, and the relative changes of the surface magnetic moment of iron in the two environments via the changes of the Fe 3*p* core hole splitting, and the changes of spin polarization. Magnetic measurements with surface sensitivity and atom specificity

were obtained by linear magnetic dichroism in the angular distribution (LMDAD) of core-level photoelectrons<sup>7-9</sup> and by spin-polarization measurements (SP) of the ejected secondary electron yield.<sup>10</sup> Photoemission dichroism originates from the specific matrix elements for photoionization of individual magnetic sublevels of the core hole in the magnetic atom.<sup>11-13</sup> The magnitude of the dichroism effect is therefore a measure of the magnetic order parameter  $\langle M \rangle$ . It can be used to measure surface sensitive, atom specific, ferromagnetic hysteresis loops  $M(H)$  as a function of the applied field  $H$ . It can also be used to study the temperature dependence  $M(T)$  of the magnetization of the surface atoms,<sup>14</sup> which is connected to the spin-wave stiffness and gives information on the exchange coupling along a path perpendicular to the surface.<sup>15,16</sup> The energy splitting of the core hole sublevels is due to the core hole spin-orbit interaction *and* to the magnetic interactions between the core hole and the spin-polarized valence band: it is reflected in the linewidth of the photoemission peak.<sup>14</sup> The core hole splitting is proportional to the local exchange interaction, i.e., it is proportional to the magnetic moment carried by the excited atom. The possibility of measuring variations of the surface magnetic moment follows from the experimental determination of the energy position of the  $\mathbf{m}j = \pm 3/2$  sublevels, which is obtained by photoemission magnetic dichroism, and is based on the assumption that the core hole splitting of these two levels varies *linearly* with the changes of the magnetic moment.<sup>12</sup> SP of the secondary electron yield provides independent measurements proportional to the surface magnetization.<sup>17</sup>

### EXPERIMENTAL

Fe(100) surfaces were prepared by Ar<sup>+</sup>-ion sputtering and annealing a [100]-oriented iron single crystal (3% silicon stabilized) mounted to close the gap of a soft iron yoke and clamped in the liquid-He-cooled manipulator of a spectrom-

eter having a residual pressure of  $2 \times 10^{-11}$  mbar. The iron single crystal could be magnetized to saturation by passing a direct current through a winding around the soft iron yoke (10 windings, 0.3 mm Ag wire). A computer controlled bipolar amplifier was used to supply current to the electromagnet in fine steps. The  $H$  field between the ribs of the yoke (in absence of the Fe single crystal) was  $\sim 10$  Oe per ampere. The  $H$ -dependent data will be presented below as a function of the magnet current. The annealing procedure needed for healing the damage induced by  $\text{Ar}^+$  bombardment, also promotes segregation of C, Si, N, and S impurities from the bulk as a function of temperature.<sup>18</sup> The clean Fe(100) surfaces were therefore obtained after a final cycle of mild sputtering and mild annealing to reduce damage and prevent segregation, or, alternatively, by homoepitaxy of Fe onto a well crystallized (but segregated) iron surface. Ordered  $c(2 \times 2)$  superstructures, corresponding nominally to 0.5 monolayers of S, could be routinely obtained after annealing above 600 °C. The S  $2p$  core level photoemission intensity was monitored during the annealing procedure which was interrupted after reaching a stationary value. S is known to replace C and Si in the fourfold hollow site of the (100) surface.<sup>18</sup> Sharp  $c(2 \times 2)$  LEED patterns were obtained and the photoemission spectra verified that only Fe and S were present at the surface. The sample temperature control was obtained by regulating the power of a W filament placed near the back face of the Fe single crystal while maintaining the flow of LHe or LN in the sample holder, according to the reading of a thin Chromel-Alumel thermocouple in contact to the sample surface.<sup>19</sup>

Photoemission magnetic dichroism of the Fe  $3p$  and S  $2p$  core levels was measured in the LMDAD mode which implies a chiral experimental geometry. The chirality of the photoemission experiments was obtained by a noncoplanar arrangement of the photon wave vector  $\mathbf{q}$ , the photoelectron wave vector  $\mathbf{p}$ , and the magnetization vector  $\mathbf{M}$  as sketched in the insets: two mirror experiments were obtained by reversing the sign of magnetization which lies always perpendicular to the scattering plane. Linearly polarized radiation in the energy range  $h\nu = 30 - 250$  eV was provided by the Swiss-French undulator beam line SU3 of the SuperAco storage ring at Orsay. An hemispherical electron energy analyzer collected photoelectrons with an angular acceptance of  $\pm 1^\circ$ , centered at  $45^\circ$  from the incoming beam direction (angle between  $\mathbf{q}$  and  $\mathbf{p}$ ). The kinetic energy of the core photoelectrons were in the range 50–80 eV, corresponding to minimal inelastic scattering length in solids. In these conditions about one third of the photoemission signal arises from surface atoms, and about one fourth from the subsurface atomic plane. The energy resolution of the Fe  $3p$  photoemission spectra (including light and analyzer bandpass) is  $100 \pm 20$  meV, of the valence-band spectra is  $40 \text{ meV} \pm 10$  meV. The magnetic asymmetry is defined as

$$A_{\text{LMDAD}} = \frac{I_{\text{up}} - I_{\text{down}}}{I_{\text{up}} + I_{\text{down}}},$$

where  $I_{\text{up}} (\text{down})$  are the photoelectron spectral intensities obtained with the magnetization in the upward (*up*) or downward (*down*) directions. SP measurements were obtained on the same sample and mounting by Mott scattering on a Au

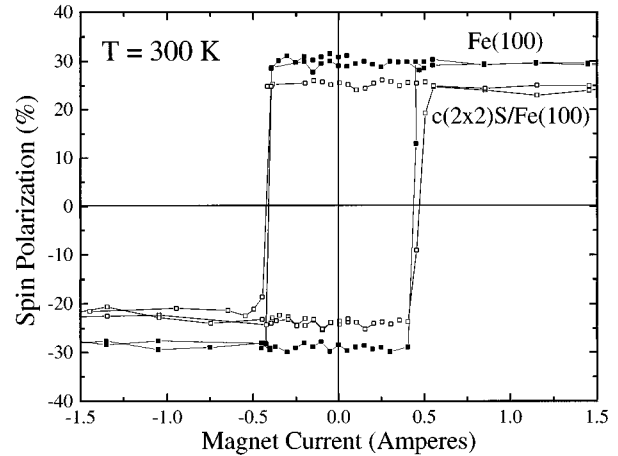


FIG. 1. Ferromagnetic hysteresis curves obtained by measuring the spin polarization (SP) of the total electron yield excited by a primary  $e$  beam of 1.5 KeV, as a function of the direct current flown into the electromagnet (proportional to the applied magnetic field  $H$ ), at room temperature, for the Fe(100) (full symbols) and for the  $c(2 \times 2)$  S/Fe(100) (open symbols) surfaces. The saturation value of the SP is defined as 1/2 the (vertical) aperture of the hysteresis loop.

foil of the total electron yield accelerated to 100 KV kinetic energy in a second UHV spectrometer with base pressure of  $7 \times 10^{-11}$  mbar, fresh surfaces were prepared following the same procedures; reproducibility of the surface quality was checked by LEED, UV-photoemission, and Auger spectroscopies. The total electron yield ejected from the sample was excited by an unpolarized primary electron beam of 1.5 KeV. The secondary electron distribution was modified by the energy bandpass of the electrostatic accelerating lens: a beam of ejected electrons with kinetic energies mostly of 5–20 eV was accelerated to the Mott scatterer. The SP is derived, via the Sherman function, from the right-left asymmetry of the scattered electron intensities with respect to the spin quantization axis in the Mott detector:<sup>20</sup>

$$A_{\text{Mott}} = \frac{I_{\text{left}} - I_{\text{right}}}{I_{\text{left}} + I_{\text{right}}}.$$

The magneto-optic Kerr effect measurements were performed *in situ* with a He-Ne laser and the technique of modulating the applied magnetic field.

## METHOD

The physical measurements upon which the present study is based are the Fe  $3p$  and S  $2p$  LMDAD photoemission spectra that were discussed in Ref. 14 and the SP magnetization curves shown in Fig. 1. Two quantities are extracted from the Fe  $3p$  LMDAD spectra: (1) the maximum asymmetry  $A_{\text{LMDAD}}$  (corresponding to the negative peak in Fig. 1 of Ref. 14), (2) the width  $W$  of the dichroism spectrum (energy interval between the positive and negative peak). Figure 1 shows the SP as a function of the applied magnetic field (direct current through the electromagnet) for Fe(100) and for the  $c(2 \times 2)$ S surface at room temperature, i.e., the ferromagnetic hysteresis loops. In the following discussion the SP data are the remanence values after application and re-

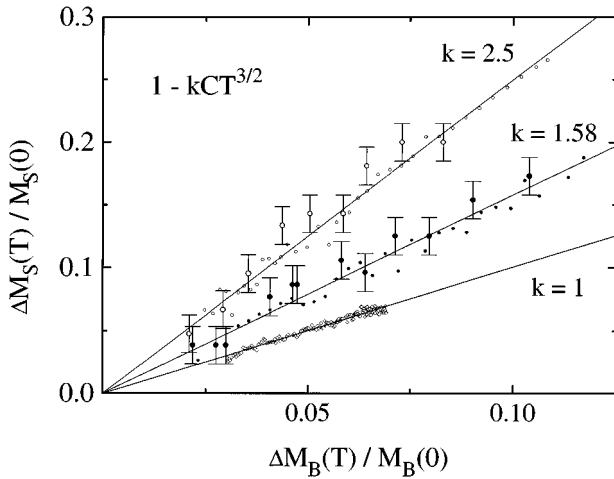


FIG. 2. Thermal decrease of the relative surface magnetization  $\Delta M_S(T)/M_S(0)$  as measured by Fe 3p LMDAD asymmetry [ $\Delta A_{\text{LMDAD}}(T)/A_{\text{LMDAD}}(0)$ , circles with error bars] and by the SP [ $\Delta \text{SP}(T)/\text{SP}(0)$ , small circles] of the secondary electron yield plotted versus the thermal decrease of the relative bulk magnetization  $\Delta M_B(T)/M_B(0)$  measured *in situ* by the magneto-optic Kerr rotation (diamonds). The open circles refer to the Fe(100) surface, the filled circles to the  $c(2 \times 2)\text{S}$  surface. The solid lines are the theoretical curves for  $k=1$ ,  $k_{\text{eff}}=1.58$ , and  $k_{\text{eff}}=2.5$ .

removal of a field pulse approximately 10 times larger than the coercive field.

## RESULTS

The temperature dependence of the photoemission dichroism and of the SP for  $T \leq 0.4T_C$ , i.e., in the spin-wave regime, is shown in Fig. 2 for both the Fe(100) and the  $c(2 \times 2)\text{S}/\text{Fe}(100)$  surfaces plotted against the temperature dependence of the bulk magnetization measured by the Kerr rotation. The LMDAD data are plotted as  $\Delta A_{\text{LMDAD}}(T)/A_{\text{LMDAD}}(0)$  and the SP data are plotted as  $\Delta \text{SP}(T)/\text{SP}(0)$ . Both these quantities are directly related to the relative variation of the surface magnetization  $\Delta M_S(T)/M_S(0)$ ; therefore both data sets are plotted in Fig. 2 as the thermal decrease of the relative surface magnetization  $\Delta M_S(T)/M_S(0)$  against the bulk thermal decrease of magnetization  $\Delta M_B(T)/M_B(0)$  (obtained from the Kerr rotation data). The results can be described by Bloch's law:  $\mathbf{M}(T)/\mathbf{M}(0) = 1 - kCT^{3/2}$ , where  $C$  is a bulk constant and  $k$  is a surface enhancement factor ( $k=1$  in the bulk).<sup>21,15</sup> The Kerr data measure the bulk thermal decrease of relative magnetization with  $k=1$  which determines experimentally the bulk constant  $C = 1.2 \times 10^{-5} (\text{degree})^{-3/2}$ .

The surface enhancement factors obtained by fitting the LMDAD and SP data to the Bloch's law for the clean Fe(100) surface and for the  $c(2 \times 2)\text{S}/\text{Fe}(100)$  surface are  $k \approx 2.5$  and  $k \approx 1.58$ , respectively. Both LMDAD and SP actually measure an effective value of  $k$  ( $k_{\text{eff}}$ ) due to the finite probing depth which is quite similar for both techniques.<sup>22</sup> In fact the best fit of the  $T^{3/2}$  law to the LMDAD data yield  $k_{\text{eff}} = 2.6$  and  $k_{\text{eff}} = 1.6$ , respectively, for the clean and sulfated surfaces, while the best fits to the SP data yield  $k_{\text{eff}} = 2.46$  and  $k_{\text{eff}} = 1.52$ , indicating a slightly

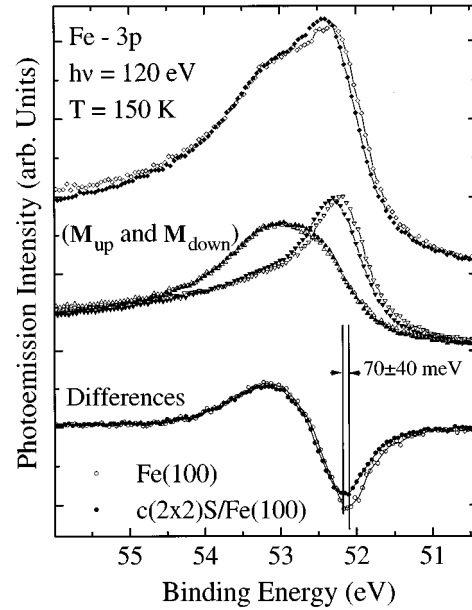


FIG. 3. Fe 3p photoemission spectra and LMDAD spectra for the clean Fe(100) surface (open symbols) and the sulfur segregated  $c(2 \times 2)\text{S}/\text{Fe}(100)$  surface (filled symbols). The reduced width of the integral spectra (diamonds) is resolved by the magnetization dependent spectra (up-down triangles, same convention as in Fig. 1). The dichroism curves (circles) show the reduced splitting of the  $j=3/2; m_j = \pm 3/2$  sublevels.

higher surface sensitivity of the photoemission data than the secondary yield data.

The Fe 3p photoemission spectra (sum, magnetization-dependent, and dichroism) for the two surfaces are compared in Fig. 3. The narrowing of the sum spectrum of the  $c(2 \times 2)\text{S}/\text{Fe}(100)$  surface relative to the Fe(100) surface is seen to arise from the shift towards higher binding energy of the spectrum measured with the magnetization "down" (i.e., along the negative y direction) whose line shape is dominated by the  $m_j = +3/2$  sublevel, which has minority spin character.<sup>9</sup> The line shapes measured with magnetization "up", which are dominated by the  $m_j = -3/2$  sublevel (of majority spin character), are similar in energy distribution and width for both surfaces. The sharp extrema of the dichroism spectrum correspond to the energy positions of the  $m_j = \pm 3/2$  sublevels which are the pure spin states of the multiplet in the simplest atomic picture.<sup>9</sup> The width  $W$  of the dichroism spectrum is interpreted as a measure of the  $m_j = \pm 3/2$  splitting, i.e., of the energy splitting due to the exchange interaction. We measure from the dichroism curves  $W_{\text{Fe}} = 1.06 \pm 0.02$  eV for clean Fe(100), and  $W_{\text{S/Fe}} = 0.99 \pm 0.02$  eV for the  $c(2 \times 2)\text{S}/\text{Fe}(100)$  surface. These data identify a "magnetochemical shift" for Fe 3p in the sulfated surface: the reduction of the  $m_j = \pm 3/2$  splitting, which amounts to  $70 \pm 40$  meV, can only be symmetrical with respect to the center of the  $j=3/2$  multiplet and the unchanged position of the  $m_j = -3/2$  spectrum can be explained by a chemical shift of the whole multiplet of 35 meV towards higher binding energies.

The SP results for the Fe(100) and for the  $c(2 \times 2)\text{S}/\text{Fe}(100)$  surfaces are plotted in Fig. 4 as a function of the sample temperature. The SP value at 150 K for the

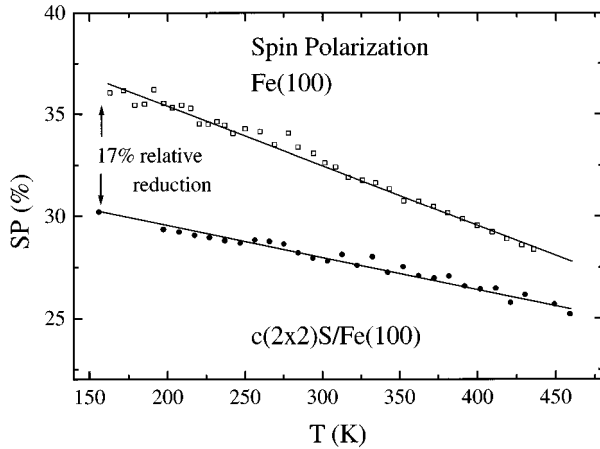


FIG. 4. Spin-polarization (SP) data for the Fe(100) (*open squares*) and  $c(2 \times 2)$ S/Fe(100) (*dots*) surfaces as a function of temperature. A relative reduction of 17% of SP is measured at 150 K for the sulfurated surface.

clean Fe(100) surface and for the  $c(2 \times 2)$ S/Fe(100) surface are 36.5% and 30% respectively, i.e., a relative reduction of SP of  $\sim 17\%$  is measured for the S segregated surface. The absolute value of the SP depends on the energy distribution of the collected electron yield, on the work function of the surface, and on the average magnetic moment of the top layers of the sample. The averaging is due to the escape depth weighted contributions of the surface, underlayer and bulk. In our experimental set up we have derived a spin-averaged escape depth for iron of  $5.85 \text{ \AA}$ .<sup>24</sup>

S  $2p$  LMDAD spectra of the  $c(2 \times 2)$ S surface of Fe(100) are shown in Ref. 14. The presence of magnetic dichroism indicates that the S  $2p$  core hole is exchange split, and therefore that a magnetic moment is transferred from Fe to S. The  $\mathbf{m}_j = \pm 3/2$  splitting of the S  $2p_{3/2}$  peak is  $\approx 450 \text{ meV}$ . The sign of the dichroism suggests that the small S magnetic moments are oriented parallel to the surface Fe moments.

Angular-resolved valence-band spectra measured with  $h\nu = 40 \text{ eV}$  at normal emission for Fe(100) and the  $c(2 \times 2)$ S/Fe(100) surfaces are compared in Fig. 5. The difference spectrum indicates the energy distribution of the S  $3p$  bands, centered at  $-4.3 \text{ eV}$ , and the intense surface state peak at  $-0.3 \text{ eV}$  below the Fermi level. Figures 6 and 7 show the LMDAD results measured on the two surfaces. Since the largest LMDAD effect on Fe(100) is measured slightly off normal emission, we selected the spectra for  $\vartheta = 10^\circ$ . The Fe(100) LMDAD spectrum shows a peak of negative asymmetry at  $-0.25 \text{ eV}$  followed at higher binding energies by a broad positive asymmetry structure. The  $c(2 \times 2)$ S LMDAD spectrum shows a very large negative asymmetry in the peak at  $-0.3 \text{ eV}$ , while the deeper structures, including the S  $3p$  bands do not show magnetic dichroism. The bottom panels of Figs. 6 and 7 display the magnetization-dependent line shapes of the valence-band spectra, as obtained after subtraction of the integral photoemission spectrum from the magnetization-dependent row spectra. This further presentation of the same data, although redundant, can be useful since the line shape of the dichroic density of states is largely hidden in the row data due to the rather small value of dichroism on valence bands. The as-

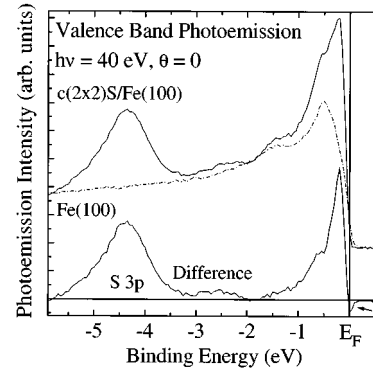


FIG. 5. Angle-resolved, normal emission, photoelectron energy distribution curves for the valence bands of Fe(100) (*dot-dashed curve*) and  $c(2 \times 2)$ S/Fe(100) (*solid curve*). The bottom spectrum is the difference curve between the sulfurated and the clean surface. It shows the S  $3p$  contribution, the sharp surface band peak at  $-0.3 \text{ eV}$  below the Fermi level, and the negative peak at the Fermi level (arrow).

segment of peaks by comparison to spin-resolved experiments and theory is easier on the subtracted data.

## DISCUSSION

### Magnetic properties

The magnetic behavior of a surface compared to the bulk of a ferromagnet, and the magnetic behavior of modified surfaces, can be described by the exchange coupling of the surface plane to the bulk, by the in-plane exchange, and by the magnetic moment of the surface atoms.

The exchange coupling of the surface atoms can be obtained by measuring the spin-wave stiffness at the surface.

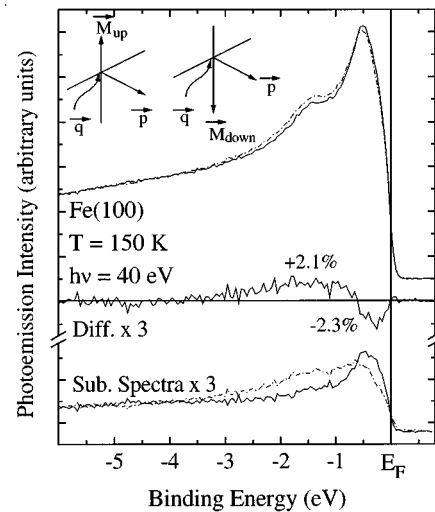


FIG. 6. LMDAD photoemission of the valence band of Fe(100) at  $\vartheta = 10$  degrees off normal emission. The dichroism is shown by the difference curve with the extrema of the asymmetry values. The bottom curves are the magnetization-dependent line shapes obtained by subtracting a magnetically averaged spectrum from the magnetization dependent spectra. The sharp peak of the continuous line (bottom curves) compare well with the minority-band peak measured with spin-resolved photoemission (Ref. 26).

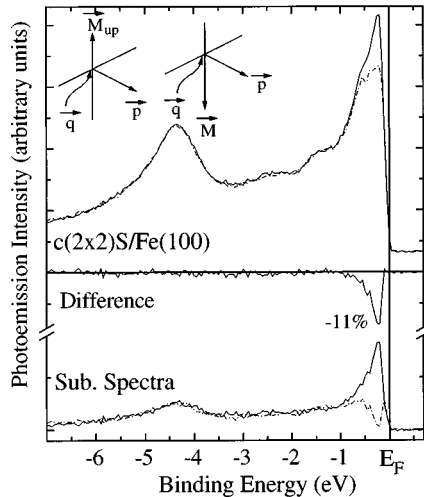


FIG. 7. LMDAD photoemission of the valence band of the  $c(2 \times 2)S/Fe(100)$  surface at normal emission. The dichroism is shown by the difference curve with the asymmetry values. The bottom curves are the magnetization-dependent line shapes obtained by subtracting a magnetically averaged spectrum from the magnetization-dependent spectra. The sharp peak of the continuous line at  $-0.3$  eV compare well with the minority-band peak measured with spin-resolved photoemission (Ref. 4).

The classical results from Rado<sup>21</sup> for the temperature dependence of an ideal surface in the range  $0.03T_C < T < 0.4T_C$  is the  $M_S(T)/M_S(0) = 1 - kCT^{3/2}$  law with  $k=2$  representing the fact that the surface is a free end for the standing spin waves and the spin-wave probability at the surface is twice that in the bulk. Mathon and Ahmad<sup>15</sup> and Scholl *et al.*<sup>16</sup> have demonstrated that enhancement factors  $k > 2$  are directly related to the reduction of the exchange coupling of the top atomic layer(s) to the bulk. The photoemission and SP measurements provide effective values of the coefficient  $k$  ( $k_{\text{eff}}$ ) which are the sum of surface ( $\sim 30\%$  of the signal) and subsurface contributions. The ideal case of  $k=2$  at the surface would therefore yield  $k_{\text{eff}} = 1.30$  in our experiment. If the change of spin-wave stiffness is limited to the surface plane then the data for Fe(100) give  $k_{\text{surf}} \approx 5.5$  which implies a reduction of the exchange perpendicular to the Fe(100) surface by a factor of 10 with respect to the bulk exchange.<sup>15</sup> The data for the  $c(2 \times 2)S/Fe(100)$  surface, in the same hypothesis, give  $k_{\text{surf}} \approx 2.75$ . These values must be considered as upper limits for the reduction of the surface perpendicular exchange since second layer softening could also exist, but cannot be discriminated. The temperature dependence of the relative magnetization in the spin-wave regime indicates therefore that (a) the clean Fe(100) surface is weakly magnetically coupled to the bulk, and (b) the exchange coupling of the top Fe layer of the sulfurated surface, while still reduced with respect to bulk Fe, is stronger than in the clean surface case. This result suggests that the overlap of the spin-polarized surface bands and bulk bands is larger in presence of S than for the clean surface.

A 35% enhancement of the (100) surface iron magnetic moment ( $\mu_{\text{surf}}$ ) with respect to the bulk value has been predicted<sup>23</sup> along with much smaller changes for the second and third atomic layers. Direct measurements of  $\mu_{\text{surf}}$  still lack. The magnetochemical shift observed on the Fe  $3p$  pho-

toemission spectra between the  $c(2 \times 2)S$  surface and the (100) surface reflects the different electrostatic *and* exchange interactions of the surface iron atoms in the two environments. The chemical shift of  $\sim 35$  meV towards higher binding energies is consistent with a small charge transfer from Fe to S. The different width  $W$  of the magnetic dichroism curve for the  $3p$  core levels of iron atoms at the  $c(2 \times 2)S$  surface ( $\Delta W/W_{\text{Fe}} \approx -7\%$ ) with respect to the clean (100) surface means a different magnetic moment of the iron atoms in the two surfaces. If the difference of magnetic moment of iron in the two environments is limited to the surface layer (representing  $\sim 30\%$  of the Fe  $3p$  photoemission intensity) the measured narrowing of the dichroism curve would imply a reduction of  $\mu_{\text{surf}}$  of  $\sim 20\%$  in the  $c(2 \times 2)S$  surface compared to the Fe(100) surface.

In order to analyze quantitatively the SP data one has to remember the fact that the results are an average of surface and subsurface contributions (which we approximate to the bulk contribution). As mentioned above the probing depth of the secondary electron yield measured by our apparatus in Fe is  $5.85 \text{ \AA}$ .<sup>24</sup> We should note here that independent evidence of this small value of the probing depth of secondary electrons in iron is given by the very similar  $k_{\text{eff}}$  values obtained from the temperature dependence data of SP and LMDAD. The Mott scattering data at 150 K (lowest temperature attained in the SP experiment) show a relative decrease of SP of 17% for the  $c(2 \times 2)S$  surface. The  $\sim 20\%$  reduction of the iron  $\mu_{\text{surf}}$  of the  $c(2 \times 2)S$  surface, deduced as an upper value from the measured LMDAD splitting, could explain a relative reduction of SP of the order of 8% with respect to the clean Fe(100) surface, due to averaging of surface and bulk contributions. The  $\sim 17\%$  SP reduction which is actually measured is therefore due not only to the reduction of the iron  $\mu_{\text{surf}}$  but also to the scattering of the spin-polarized secondary electrons on the sulfur atoms, to the sulfur contribution to the secondary yield, and to the  $\sim 0.5$  eV increase of the work function.<sup>2</sup>

Qualitatively the LMDAD and SP results are consistent. It is nevertheless clear that the number of parameters responsible for a change of SP of the secondary yield is large and a more stringent quantitative comparison of the results would require accurate measurements of SP attenuation crossing a S layer, of the secondary yield of S and of the spin-filtering effect of a surface layer having high  $\mu_{\text{surf}}$ .<sup>24,25</sup> The upper limit of the reduction of the iron  $\mu_{\text{surf}}$  set by the LMDAD experiment is a smaller value than it could be guessed from an oversimplified analysis of the reduction of SP alone. The  $\sim 20\%$  reduction of the iron  $\mu_{\text{surf}}$  of the  $c(2 \times 2)S$  surface roughly compensates the surface enhancement of the iron magnetic moment of the clean (100) surface. Again this implies a larger overlap of surface and bulk electron bands at the sulfurated surface.

### Electron states

The large magnetic changes that the Fe(100) surface undergoes upon segregation of S in the  $c(2 \times 2)S$  reconstruction are the consequence of the electron states determined by the bonding of the iron surface atoms with S. S atoms occupy the fourfold surface sites at a height of about  $1.1 \text{ \AA}$  above the surface, establishing S-Fe bond lengths of  $2.30$

Å.<sup>1</sup> As seen from the very small negative shift of the Fe 3*p* core levels the charge transfer from Fe to S is small. Yet the changes of the (spin-polarized) electron state distribution are large and easily observed in the angular-resolved photoemission spectra. Several previous ARPES (Ref. 3) and spin-resolved ARPES (Ref. 4) studies have shown the presence of exchange splitting in the S 3*p* valence bands and of spin-polarized surface resonances connected with the bonding of iron with sulfur. The augmented plane-wave calculations of the band structure of *c*(2×2)S/Fe(100) by Chubb and Pickett<sup>6</sup> show that the hybridization of the surface iron bands with the S 3*p* bands implies the broadening of the majority *d* band with a loss of charge, and the filling of the minority *d* band, along with an overall decrease of density of states at the Fermi level. These theoretical results predicted in particular a reduction of the iron  $\mu_{\text{surf}}$  well confirmed by the present results.

The band-structure features induced by the reconstruction on the Fe(100) surface are reflected in the normal emission spectra of the two surfaces which are compared in Fig. 5. The S 3*p* main peak is found at -4.4 eV, further peaks appear at -2.5 and -1.4 eV, and a large peak is found at -0.3 eV below the Fermi level. The density of states at the Fermi level is reduced in the *c*(2×2)S spectrum with respect to the clean surface. These spectral features indicate that the *d* band of Fe is heavily hybridized with the S 3*p* states throughout the whole bandwidth. The peak near the Fermi level in the LMDAD-subtracted spectra of Fe(100) (measured at 10° off normal emission) identified by the negative dichroism asymmetry, corresponds in energy, to the minority-spin band ( $\Gamma_{25}^{\downarrow}$ ) which is well documented by spin-resolved ARPES.<sup>26,27</sup> The LMDAD-subtracted spectra of the *c*(2×2)S surface show that the very intense peak at -0.3 eV below the Fermi level has the same sign of dichroism as in the Fe(100) case. Its increased intensity can therefore be interpreted as due to the filling of the minority-spin band of iron due to hybridization with sulfur; this is consistent with spin-resolved photoemission data<sup>4</sup> and with theoretical predictions.<sup>6</sup> The valence-band spectra give therefore evidence of changes in the spin-polarized density of states at the *c*(2×2)S surface that imply both the broadening of the surface iron *d* band and the filling of the minority-spin band. These results give a qualitative account of the magnetometric results: (1) the filling of the minority-spin surface band of iron determines the reduced surface magnetic moment of the iron surface atoms bonded to sulfur; (2) the broadening of the iron surface density of states in presence of sulfur deter-

mines an increased overlapping of surface and bulk bands and consequently a stronger exchange coupling along a path perpendicular to the surface.

LMDAD in valence-band states is not an alternative technique to spin-polarized photoemission since magnetic dichroism is not expected for strongly hybridized band states, and the sign cannot be firmly predicted. It is nevertheless clear that the existence of narrow bands highly spin polarized is reflected in large signals in the photoemission magnetic dichroism experiment.<sup>28</sup> Based on this empirical consideration one should note that the exchange splitting of the S 3*p* bands, documented by spin-resolved photoemission experiments,<sup>4</sup> is not revealed by photoemission dichroism, probably indicating that the S 3*p* states are strongly hybridized between -3.5 and -6 eV below the Fermi level.

## CONCLUSIONS

Sulfur segregation heavily modifies the surface magnetic properties of Fe(100): (1) The magnetic coupling of the *c*(2×2)S/Fe(100) surface to the bulk is two times stronger than for the Fe(100) surface. This can be explained by the broadening of the surface iron *d* bands due to the hybridization with the S 3*p* bands which involves first and second layer Fe atoms. (2) The magnetic moment of the surface iron atoms is reduced by up to 20% in the *c*(2×2)S surface with respect to the clean Fe(100) surface. This is consistently measured by LMDAD and SP and can be connected with the filling of the surface minority-spin band observed in the (dichroic) density of states below the Fermi level of the *c*(2×2)S/Fe(100) surface. (3) As a consequence of the S 3*p* hybridization a magnetic moment is transferred to the sulfur atoms as seen by the presence of LMDAD signal of the S 2*p* core levels. The magnitude of the S magnetic moment cannot be estimated on the basis of our data, but the sign of the photoemission dichroism indicates a parallel alignment with the iron surface momenta determining an overall ferromagnetic order of the *c*(2×2)S/Fe(100) surface bilayer.

## ACKNOWLEDGMENTS

Thanks are due to H.C. Siegmann for continuous support and discussion and to E. Narducci for help with the experiments. This work was partially supported by the Swiss National Fund and by the EC Human Capital and Mobility program.

<sup>1</sup>K.O. Legg, F. Jona, D.W. Jepsen, and P.M. Marcus, *Surf. Sci.* **66**, 25 (1977).

<sup>2</sup>K. Ueda and R. Shimizu, *Jpn. J. Appl. Phys.* **12**, 1869 (1973).

<sup>3</sup>R.A. DiDio, E.W. Plummer, and W.R. Graham, *Phys. Rev. Lett.* **52**, 683 (1984).

<sup>4</sup>P.D. Johnson, A. Clarke, N.B. Brookes, S.L. Hulbert, B. Sinkovic, and N.V. Smith, *Phys. Rev. Lett.* **61**, 2257 (1988); A. Clarke, N.B. Brookes, P.D. Johnson, M. Weinert, B. Sinkovic, and N.V. Smith, *Phys. Rev. B* **41**, 9659 (1990).

<sup>5</sup>G. Schonhense, M. Getzlaff, C. Westphal, B. Heidemann, and J.

Bansmann, *J. Phys. (Paris) Colloq.* **49**, C8-1643 (1988).

<sup>6</sup>S.R. Chubb and W.E. Pickett, *Phys. Rev. B* **38**, 10 227 (1988).

<sup>7</sup>Ch. Roth, F.U. Hillebrecht, H. Rose, and E. Kisker, *Phys. Rev. Lett.* **70**, 3479 (1993); *Solid State Commun.* **86**, 647 (1993).

<sup>8</sup>F. Sirotti and G. Rossi, *Phys. Rev. B* **49**, 15 682 (1994).

<sup>9</sup>G. Rossi, F. Sirotti, N. Cherepkov, F. Combet Farnoux, and G. Panaccione, *Solid State Commun.* **90**, 557 (1994); G. Rossi, F. Sirotti, and G. Panaccione, in *Core Level Spectroscopies For Magnetic Phenomena: Theory and Experiment*, Vol. 345 of NATO ASI Series B: Physics, edited by P.S. Bagus, G. Pac-

- chioni, and F. Parmigiani (Plenum, New York, 1995) p. 181; G. Rossi, G. Panaccione and F. Sirotti, in *Magnetic Ultrathin Films, Multilayers and Surfaces*, edited by E. E. Marinero *et al.*, MRS Symposia Proceedings No. 384 (Materials Research Society, Pittsburgh, 1995), p. 447.
- <sup>10</sup>H.C. Siegmann, D. Mauri, D. Scholl, and E. Kay, *J. Phys. (Paris) Colloq.* **49**, C8-9 (1988).
- <sup>11</sup>N.A. Cherepkov, *Phys. Rev. B* **50**, 13 813 (1994).
- <sup>12</sup>G. van der Laan, *Phys. Rev. B* **51**, 240 (1995).
- <sup>13</sup>E. Tamura, G.D. Waddill, J.G. Tobin, and P.A. Sterne, *Phys. Rev. Lett.* **73**, 1533 (1994).
- <sup>14</sup>F. Sirotti, G. Panaccione, and G. Rossi, *Phys. Rev. B* **52**, R17 063, (1995); G. Panaccione, F. Sirotti, and G. Rossi, *J. Electron Spec. Relat. Phenom.* **76**, 189 (1995).
- <sup>15</sup>J. Mathon and S.B. Ahmad, *Phys. Rev. B* **37**, 660 (1988); J. Mathon, *Physica B* **149**, 31 (1988).
- <sup>16</sup>D. Mauri, D. Scholl, H.C. Siegmann, and E. Kay, *Phys. Rev. Lett.* **61**, 758 (1988); D. Scholl, M. Donath, D. Mauri, E. Kay, J. Mathon, R.B. Muniz, and H.C. Siegmann, *Phys. Rev. B* **43**, 13 309 (1991).
- <sup>17</sup>H.C. Siegmann, *J. Phys. Condens. Matter* **4**, 8395 (1992).
- <sup>18</sup>F. Jona and J.A. Strozier, in *Epitaxial Growth*, edited by J.W. Matthews (Academic, New York, 1975).
- <sup>19</sup>G. Panaccione, Ph.D. thesis, University Pierre et Marie Curie, Paris, 1995.
- <sup>20</sup>J. Kessler, *Polarized Electrons* (Springer-Verlag, Berlin, 1976).
- <sup>21</sup>G.T. Rado, *Bull. Am. Phys. Soc. II* **2**, 127 (1957).
- <sup>22</sup>O. Paul, Ph.D. thesis, ETH Zurich, 1993.
- <sup>23</sup>S. Onishi, A.J. Freeman, and M. Weisert, *Phys. Rev. B* **28**, 6741 (1983).
- <sup>24</sup>F. Sirotti, G. Panaccione, and G. Rossi, *J. Phys. (Paris) Colloq.*, **55**, C9-175 (1994).
- <sup>25</sup>H.C. Siegmann, in *Core Level Spectroscopies for Magnetic Phenomena: Theory and Experiment* (Ref. 9), p. 1.
- <sup>26</sup>E. Kisker, K. Schroder, W. Gudat, and M. Campagna, *Phys. Rev. B* **31**, 329 (1985).
- <sup>27</sup>N.B. Brookes, A. Clarke, P.D. Johnson, and M. Weinert, *Phys. Rev. B* **41**, 2643 (1990).
- <sup>28</sup>M. Getzlaff, Ch. Ostertag, G.H. Fecher, N.A. Cherepkov, and G. Schönhense, *Phys. Rev. Lett.* **73**, 3030 (1994).